Redox-Dependent ^{1}H NMR Spectral Features and Tertiary Structural Constraints on the C-Terminal Region of Putidaredoxin†

Thomas C. Pochapsky,* Gayathri Ratnaswamy, and Alexandra Patera

Department of Chemistry, Brandeis University, Waltham, Massachusetts 02254-9110

Received December 16, 1993; Revised Manuscript Received March 23, 1994®

ABSTRACT: Putidaredoxin (Pdx) is a 106-residue Fe_2S_2 ferredoxin which acts as the physiological reductant and effector of cytochrome P-450$_{cam}$. Pdx has two accessible oxidation states, Fe^{+3}–Fe^{+3} (oxidized) and Fe^{+3}–Fe^{+2} (reduced), and exhibits redox-dependent binding affinities for cytochrome P-450$_{cam}$, with reduced Pdx binding over 100-fold more tightly than oxidized Pdx to the oxidized cytochrome P-450$_{cam}$ [Hintz, M. J., Mock, D. M., Peterson, L. L., Tuttle, K., & Peterson, J. A. (1982) *J. Biol. Chem. 257*, 14324-14332]. The analysis of two-dimensional ^{1}H NMR experiments has yielded sequential ^{1}H resonance assignments for the diamagnetic regions of the reduced form of Pdx, which are compared to those of oxidized Pdx, described previously [Ye, X. M., Pochapsky, T. C., & Pochapsky, S. S. (1992) *Biochemistry 31*, 1961–1968]. Increased unpaired electron-spin density on the metal cluster in reduced relative to oxidized Pdx increases the number of ^{1}H resonances which are broadened by the metal cluster, and the pattern of paramagnetic broadening provides information concerning the placement of the metal cluster within the protein. Two-dimensional exchange experiments on half-reduced samples of Pdx indicate that electron self-exchange is slow on the chemical shift time scale, with a second-order rate constant ≤ 66 M^{-1} s^{-1} at 290 K. Spectral changes unrelated to increases in unpaired electron-spin density are also observed. The largest changes of this type are observed for features structurally contiguous with the C-terminal region Pro 102–Trp 106. The C-terminal residue Trp 106 has been implicated in binding to cytochrome P-450$_{cam}$. NOE constraints on the structure of this region are described, and a model for the solution structure of Pdx is used to rationalize the observed paramagnetic broadening patterns. A hypothesis is offered to rationalize observed redox-state-dependent binding of Pdx to P-450$_{cam}$ and changes in midpoint potential of oxidized Pdx upon binding to oxidized P-450$_{cam}$.

Living systems contain well-defined chemical potential gradients that are maintained for the most part with free energy released by tightly regulated redox reactions. Both spatial and temporal regulation of these redox reactions are required in order to prevent equilibration across chemical gradients. Biological regulation of electron transfer is typically achieved by physically isolating redox centers within protein matrices and regulating interaction between the proteins. Only if the appropriate protein–protein interactions occur will electron transfer take place (McLendon, 1988).

The putidaredoxin (Pdx)[1]/P-450$_{cam}$ system is one of the best characterized of any biological redox coupling. The crystal structure of P-450$_{cam}$ was, until recently, the only structure published for this family of enzymes (Poulos et al., 1987; Ravichandran et al., 1993), and a wealth of kinetic, mechanistic, and thermodynamic data is available concerning the camphor monooxygenase system (Sligar & Murray, 1986). Now, the use of NMR structural methods has permitted us to describe a model for the solution structure for the oxidized protein (Pochapsky & Ye, 1991; Ye et al., 1992; Pochapsky et al., 1994). It has been observed that reduced Pdx has at least a 100-fold higher binding affinity for oxidized P-450$_{cam}$ than does oxidized Pdx (Hintz et al., 1982). Conversely, P-450$_{cam}$-bound Pdx is more readily reduced ($\Delta E_o' = -196$ mV) than free Pdx ($\Delta E_o' = -230$ mV) (Sligar & Gunsalus, 1976). In an effort to clarify the relationship between oxidation state and structure/function in Pdx, we have sequentially assigned the diamagnetic portions of the ^{1}H spectrum of reduced Pdx and related the observed spectral differences between the oxidized and reduced proteins to the model for the solution structure of Pdx presented in the accompanying paper, as well as related the differences to what is known concerning the specific interactions between Pdx and P-450$_{cam}$. A similar (although less extensive) comparison between the oxidized and reduced forms of a related ferredoxin, mammalian adrenodoxin, was described by Miura (Miura & Ichikawa, 1991). We have also investigated the kinetics of electron self-exchange, using half-reduced samples of Pdx by observing exchange cross peaks in NOESY spectra as a function of mixing time.

Particularly relevant to an understanding of specific interactions between Pdx and P-450$_{cam}$ are the tertiary structural constraints on the C-terminal region of Pdx. The C-terminal residue, Trp 106, has been shown to be required for productive binding of the two proteins and is transferred from an aqueous to a nonpolar environment upon complex formation (Sligar et al., 1974; Davies et al., 1990; Davies & Sligar, 1992). As such, Trp 106 provides a structural marker for the P-450-binding surface of Pdx. We, herein, detail structural constraints on the C-terminal region of Pdx and

† This work was supported by a grant from the National Institutes of Health (GM-44191). T.C.P. gratefully acknowledges support by the NSF Young Investigator and the Camille and Henry Dreyfus Teacher–Scholar programs.

* To whom correspondence should be addressed.

® Abstract published in *Advance ACS Abstracts,* May 1, 1994.

[1] Abbreviations: CS, conformational substate; DQF-COSY, double-quantum-filtered correlation spectroscopy; DQ, double-quantum spectroscopy; DSS, 2,2-dimethyl-2-silapentane-5-sulfonate; FAD, flavin adenine dinucleotide; fid, free induction decay; HOHAHA, homonuclear Hartmann–Hahn experiment; NADH, nicotinamide adenine dinucleotide; NMR, nuclear magnetic resonance; NOE, nuclear Overhauser effect; NOESY, two-dimensional NOE spectroscopy; Pdx, putidaredoxin; rf, radio frequency.

0006-2960/94/0433-6433$04.50/0

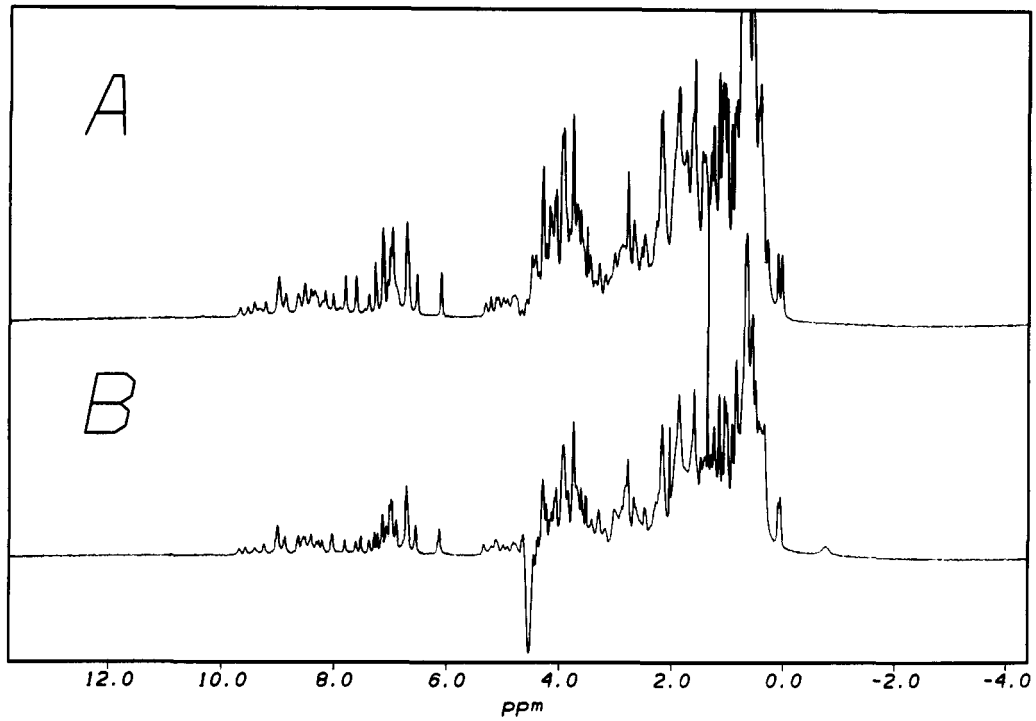

FIGURE 1: 500.13-MHz ^1H NMR spectrum of (A) oxidized and (B) reduced Pdx, 2 mM in ^2H_2O, pH 7.4, 290 K. Chemical shifts are referenced to external DSS. Note the appearance of a broadened resonance, integrating to three protons, at –0.8 ppm in the reduced protein. This (unidentified) resonance is used as a marker for complete reduction.

describe structural features that are likely to be located in or near the protein–protein interface in the diprotein complex.

MATERIALS AND METHODS

Oxidized Pdx was obtained from bacterial cultures and purified as described previously (Pochapsky & Ye, 1991). After purification, buffer was exchanged for an argon-purged 90%/10% mixture of H_2O and D_2O, which was buffered with 0.05 M Tris-d_6 at pH 7.4. Buffer exchange was accomplished on a centrifugally forced column packed with preequilibrated P-2 size exclusion gel (BioRad). The sample (typically 4 mM) was then placed in a septum-sealed 5-mm NMR tube and the tube purged with argon.

A 0.1 M sodium dithionite solution was prepared by placing the appropriate amount of fresh sodium dithionite in a vial that was then septum-sealed and purged with argon. The appropriate amount of argon-purged buffer identical to that used for NMR sample preparation was then introduced by syringe into the vial and the resulting solution purged with argon for several minutes. A microliter syringe was used to titrate the sample in the NMR tube with the dithionite solution. The integration of a broad peak near –0.8 ppm, corresponding to three protons, is a useful NMR marker for complete reduction (Figure 1). All NMR spectral changes described herein are reversible and correspond precisely with reduction, as determined spectrophotometrically (Cushman et al., 1967).

NMR experiments were performed on either a Bruker AMX-500 spectrometer operating at 500.13 MHz (Brandeis University) or a Bruker AMX-600 spectrometer operating at 600.14 MHz (Bruker Institute, Billerica, MA). A ^1H spectral width of 8064 Hz was used for experiments on the AMX-500 spectrometer, while a spectral width of 10 000 Hz was used on the AMX-600 spectrometer. Water suppression was obtained in all cases by presaturation. A digital resolution of 2048 complex points was routinely used in the ω_2 dimension. A total of 400 t_1 increments was used for NOESY, 2Q, and HOHAHA experiments, while 500 t_1 increments were used for 2QF-COSY experiments. Quadrature detection and phase sensitivity in t_1 in all experiments were obtained using time-proportional phase incrementation (TPPI). The NOESY experiment was performed using a standard sequence with a mixing time of 100 ms (Billeter et al., 1982; Kumar et al., 1980). The same sequence was used to characterize electron self-exchange in half-reduced samples of Pdx. The 2QF-COSY experiment was also obtained with a standard sequence (Rance et al., 1983). The HOHAHA experiment was run using a standard sequence (Bax & Davis, 1985) but with very short (2.5 μs) trim pulses before and after the spin–lock mixing time. An MLEV-17 sequence was used for spin–locking, with rf amplitude adjusted for a 7.5-kHz precessional frequency in the rotating frame.

The phase-sensitive DQ experiment was obtained using the sequence of Rance (Rance et al., 1989). A double-quantum mixing time of 22.5 ms was used without presaturation during mixing in order to prevent the bleaching of correlations with resonances under the water line. A sweep width of 20 000 Hz was used in t_1 for this experiment on the AMX-600 spectrometer. Nonselective ^1H T_1 values for Trp 106 indole resonances were measured in ^2H_2O solution using a standard inversion-recovery sequence, with 12–16 different delay times between the inversion and read pulses. Signal intensities as a function of interpulse delay were fitted to a single exponential curve in order to calculate relaxation rate constants.

Two-dimensional NMR data were processed using the FELIX 2.10 software package (Biosym Technologies) operating on a Silicon Graphics IRIS 4D/35 workstation. Data sets were routinely zero-filled to 2048 real points in the t_1 dimension prior to transformation. A 45° phase-shifted sine bell was applied to free induction decays obtained for 2QF-COSY and DQ experiments prior to transformation. A Gaussian window function was used for resolution enhancement prior to transformation of NOESY and HOHAHA data. The first data point of all free induction decays was multiplied by 0.5 prior to transformation in t_2, while the first data set

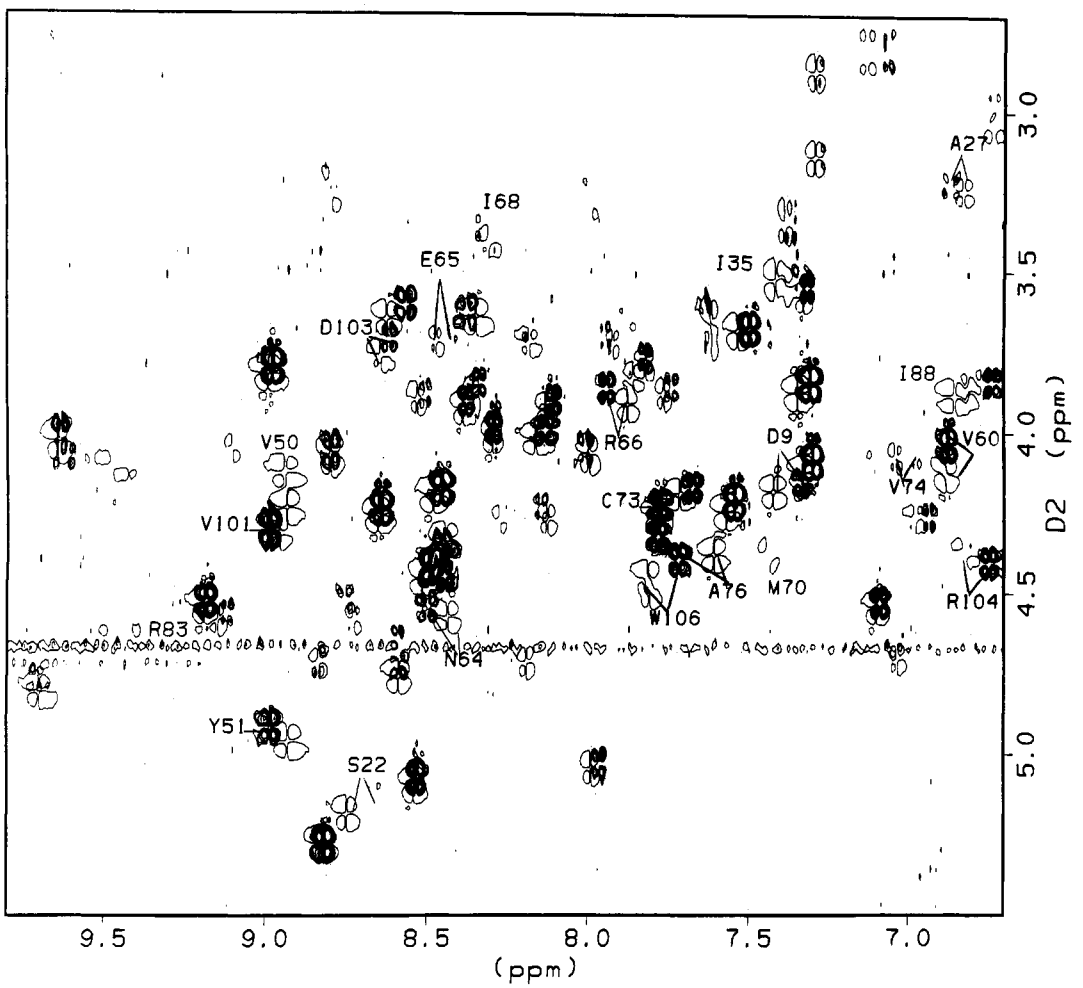

FIGURE 2: Comparison of the NH–C_αH fingerprint regions of the 600.14-MHz ^{1}H DQF-COSY spectra of oxidized and reduced Pdx. The oxidized spectrum is shown with a single contour, while the reduced protein is plotted with five contours. Only those resonances which differ significantly between the oxidized and reduced protein are identified by sequence number and the single-letter amino acid code. The sequence of Pdx is as follows: SKVVYVSHDGTRRQLDVADGVSLMQAAVSNGIYDIVGDCGGSASCATCHVYVNEAFTDKVPAANEREIG-MLECVTAELKPNSRLCCQIIMTPELDGIVVDVPDRQW (Koga et al., 1989).

(t_1 = 3 μs) was multiplied by 0.5 in cosine-modulated experiments (NOESY, HOHAHA) prior to transformation in t_1 in order to reduce t_1 noise (Otting et al., 1986). A polynomial base-line straightening routine was also applied to NOESY and TOCSY data in ω_2 prior to t_1 transformation.

Structural models for oxidized Pdx were generated using a modified version of the X-PLOR simulated annealing protocol of Nilges et al. (Nilges et al., 1988). These calculations are described in detail in the accompanying paper (Pochapsky et al., 1994). Models for the reduced protein were generated in a similar fashion. The lack of large changes in chemical shift and NOE intensities for most of the protein was taken as evidence that the structure of most of the protein is relatively unperturbed by changes in oxidation state (see Figure 2). Therefore, except for those constraints specifically noted in Table 2, NOE and dihedral angle constraints were kept the same as for the oxidized protein (see accompanying paper). Figure 5 was generated using the MOLSCRIPT program (Kraulis, 1991).

RESULTS

The assignment of the ^{1}H spectrum of reduced Pdx was for the most part straightforward; the assignments of many resonances are unchanged or only slightly different from those of oxidized Pdx, and a direct comparison between the previously assigned oxidized and reduced spectra was sufficient to make sequence-specific assignments in the reduced form in most cases (Figure 2). The methodology used for sequential assignment has been described in detail elsewhere (Wüthrich, 1986), and the application of these methods to the assignment of oxidized Pdx has also been detailed (Ye et al., 1992). The results of the assignment process for reduced Pdx are summarized in Table 1.

Differences in Hyperfine Broadening of ^{1}H Resonances between the Oxidized and Reduced Pdx. The most apparent spectral difference between the oxidized and reduced forms of Pdx is the decrease in the number of resonances observed in two-dimensional NMR experiments due to hyperfine broadening in the reduced protein. The line broadening due to paramagnetic effects drops off as an inverse sixth power of the distance between the observed spin and the paramagnetic center (Phillips & Poe, 1973). In the oxidized form, the metal cluster of Pdx is diamagnetic at low temperatures due to antiferromagnetic coupling of the two $S = {}^5/_2$ iron atoms, which results in a manifold of electronic states with net spins ($S'=0, S'=1, S'=2, S'=3,...$) separated by energy spacings ($J, 2J, 3J,...$, where J is the isotropic coupling constant between the two electronic spins) (Banci et al., 1990). J is on the order of kT at 290 K, so states with $S > 0$ are thermally populated under the conditions of the present experiments in oxidized Pdx (Ratnaswamy & Pochapsky, 1993). In the reduced form, the resulting manifold is $S' = {}^1/_2$, $S' = {}^3/_2$, $S' = {}^5/_2$, $S' = {}^7/_2$,..., spaced by ${}^3/_2J, {}^5/_2J, {}^7/_2J,...$ All populated states in the

Table 1: ^{1}H Resonance Assignments for Reduced Pdx, pH 7.4, 17 °C[a]

residue	assignment
**His 8	NH 7.51; $C_\alpha H$ 4.21; $C_\beta H_2$ 3.05 (3.10), 2.82 (2.90); $C_{\delta 2} H$ 7.04 (7.15); $N_{\delta 1} H$ 9.46; $C_{\epsilon 1} H$ 8.02 (7.92)
*Asp 9	NH 7.33 (7.41); $C_\alpha H$ 4.16; $C_\beta H_2$ 2.73, 2.04 (2.09)
*,***Arg 13	NH 8.44 (8.49); $C_\alpha H$ 4.44; $C_\beta H_2$ 1.66, 1.69; $C_\gamma H_2$ 1.29, 1.51; $C_\delta H_2$ 2.97, 2.92 (3.02); ($N_\epsilon H$ 6.74; $N_{\eta 1} H_2$ 6.23; $N_{\eta 2} H_2$, 7.20)
*,***Ser 22	NH 8.66 (8.75); $C_\alpha H$ 5.12 (5.18); ($C_\beta H_2$ 3.69, 4.08)
***Leu 23	(NH 8.38; $C_\alpha H$ 3.90); [$C_\beta H_2$ 1.70, 1.85]; $C_\gamma H$ 1.68; $C_\delta H_3$ 0.57; $C_{\delta'} H_3$ 0.52
***Gln 25	($C_\alpha H$ 3.63); $C_\beta H_2$ 1.80; $C_\gamma H_2$ 2.34; $N_\epsilon H_2$ 7.6, 6.34
*Ala 27	NH 6.87 (6.81); $C_\alpha H$ 3.22; $C_\beta H_3$ 1.08
*,***Val 28	NH 8.22; $C_\alpha H$ 3.71; $C_\beta H$ 1.85 (1.90); $C_\gamma H_3$ [0.70 (0.75)]; $C_{\gamma'} H_3$ 0.68
*Asn 30	NH 7.04; $C_\alpha H$ 4.69; $C_\beta H_2$ 2.60, 2.28; $N_\delta H_2$ 7.04, 8.46 (8.41)
**Asp 34	NH 9.62 (9.47); $C_\alpha H$ 4.08; $C_\beta H_2$ 2.45, 2.52
*,***Ile 35	NH 7.46 (7.41); ($C_\alpha H$ 3.50); $C_\beta H$ 1.54 (1.39); $C_{\gamma 2} H_3$ 0.95; $C_{\gamma 1} H$ 1.04; $C_{\gamma 2} H$ 2.11; $C_{\delta 1} H_3$ 0.39
**His 49	$C_{\epsilon 1} H$ 7.22; $N_{\delta 1} H$ 11.90 (12.01); $C_{\delta 2} H$ 10.06 (10.12)
***Val 50	(NH 8.92; $C_\alpha H$ 4.12); $C_\beta H$ 1.79; ($C_\gamma H_3$ 0.71); $C_{\gamma'} H_3$ 0.38
*Tyr 51	NH 8.98 (8.92); $C_\alpha H$ 4.91 (4.96); $C_\beta H_2$ 2.70, 2.66; $C_\delta H_2$ 6.62; $C_\epsilon H_2$ 6.64
*Val 52	NH 8.61; $C_\alpha H$ 3.59; $C_\beta H$ 1.86; $C_\gamma H_3$ 0.79; $C_{\gamma'} H_3$ 0.61 (0.66)
*Glu 54	NH 9.04 (9.09); $C_\alpha H$ 4.03; $C_\beta H_2$ 1.84 (1.90); $C_\gamma H_2$ 2.12
*Val 60	NH 6.88; $C_\alpha H$ 4.04 (4.11); $C_\beta H$ 1.81 (1.86); $C_\gamma H_3$ 0.84; $C_{\gamma'} H_3$ 0.78
*Ala 63	NH 8.51; $C_\alpha H$ 3.88; $C_\beta H_3$ 0.96 (1.01)
*,***Asn 64	NH 8.50 (8.45); $C_\alpha H$ 4.54; $C_\beta H_2$ 3.16, 2.78; $N_\delta H_2$ (6.47), 7.48
*Glu 65	NH 8.43 (8.48); $C_\alpha H$ 3.68; $C_\beta H_2$ 1.81; $C_\gamma H_2$ 2.09
*Arg 66	NH 7.94 (7.88); $C_\alpha H$ 3.85 (3.90); $C_\beta H_2$ 1.70, 1.63; $C_\gamma H_2$ 1.52; $C_\delta H_2$ 2.99, 3.01; ($N_\epsilon H$ 6.735)
***Glu 67	(NH 8.09); $C_\alpha H$ [4.02]; ($C_\beta H_2$ 1.61; $C_\gamma H_2$ 2.00)
*Ile 68	NH 8.36 (8.29); $C_\alpha H$ 3.35 (3.40); $C_\beta H$ 1.59; $C_{\gamma 2} H_3$ 0.68; $C_{\gamma 1} H_2$ 0.87, 1.34; $C_{\delta 1} H_3$ 0.50
***Met 70	NH 7.41; ($C_\alpha H$ 4.37)
***Leu 71	(NH 8.38)
**Cys 73	NH 7.77; $C_\alpha H$ 4.23 (4.49); $C_\beta H_2$ 2.95 (3.15), 2.85
,*Val 74	NH 6.98 (7.11); $C_\alpha H$ 4.12; ($C_\beta H$ 1.68; $C_\gamma H_3$ 0.37; $C_{\gamma'} H_3$(0.68))
**Thr 75	NH 8.14; $C_\alpha H$ 3.99; $C_\beta H$ 3.68 (3.78); $C_\gamma H_3$ 0.93 (0.97)
**Ala 76	NH 7.78 (7.62); $C_\alpha H$ 4.33 (4.38); $C_\beta H_3$ 1.42
*Leu 78	NH 8.43 (8.49): $C_\alpha H$ 4.41; $C_\beta H_2$ 1.58, 1.59; $C_\gamma H$ 1.15; $C_\delta H_3$ 0.78; $C_{\delta'} H_3$ 0.63
*Lys 79	NH 9.71; $C_\alpha H$ 4.77; $C_\beta H_2$ 1.55, 1.70; $C_\gamma H_2$ 1.04, 0.93; $C_\delta H_2$ 1.71, 0.39 (0.43); $C_\epsilon H_2$ 2.12
,*Arg 83	NH 9.36; $C_\alpha H$ [4.65]; $C_\beta H_2$ 1.02, 1.05; $C_\gamma H_2$ 1.56, 1.16; $C_\delta H_2$ 3.02, 3.29 (3.08, 3.39); $N_\epsilon H$ 10.04 (10.29); ($N_{\eta 1} H_2$ 8.37; $N_{\eta 2} H_2$ 550)
***Gln 87	(NH 6.80; $C_\alpha H$ 3.85; $C_\beta H_2$ 1.91; $C_\gamma H_2$ 2.37, 2.15)
***Ile 88	(NH 6.84; $C_\alpha H$ 3.88; $C_\beta H$ 1.56; $C_{\gamma 2} H_3$ 0.47;) $C_{\gamma 1} H_2$ [0.64, 1.34]; $C_{\delta 1} H_3$ [0.35]
*,***Val 101	NH 8.98; $C_\alpha H$ 4.28 (4.23); $C_\beta H$ 1.89; ($C_\gamma H_3$ 0.72); $C_{\gamma'} H_3$ 0.56
*Pro 102	$C_\alpha H$ 4.53; $C_\beta H_2$ 2.05, 1.78 (1.72); $C_\gamma H_2$ 0.75 (0.70), 1.25 (1.20); $C_\delta H_2$ 3.63 (3.54), 2.73
*Asp 103	NH 8.62; $C_\alpha H$ 3.70 (3.76); $C_\beta H_2$ 2.12 (2.18), 1.52 (1.60)
*Arg 104	NH 6.75 (6.82); $C_\alpha H$ 4.40; $C_\beta H_2$ 1.57; $C_\gamma H_2$ 1.37 (1.31); $C_\delta H_2$ 2.77, 2.72 (2.83); $N_\epsilon H$ 7.08 (7.13)
**Gln 105	NH 8.45; $C_\alpha H$ 4.34; $C_\beta H_2$ 0.81 (0.97); $C_\gamma H_2$ 2.33, 1.58 (1.44)
**Trp 106	NH 7.71 (7.84); $C_\alpha H$ 4.39 (4.46); $C_\beta H_2$ 2.78, 3.24 (3.32); $C_{\delta 1} H$ 6.96 (7.06); $C_{\epsilon 3} H$ 7.46 (7.56); $N_{\epsilon 1} H$ 9.82 (10.04); $C_{\zeta 3} H$ 6.83 (6.90); $C_{\zeta 2} H$ 7.02 (7.20); $C_\eta H$ 6.82 (6.92)

[a] Only those spin systems for which assignments differ from those of the oxidized protein by more than 0.05 ppm are presented. Assignments are not stereospecific. A bracket indicates assignments based on NOESY data and analogy with the oxidized protein. An asterisk indicates a difference of 0.05 ppm or larger is observed between the oxidized and reduced assignments for a given residue. A double asterisk indicates a difference of 0.10 ppm or greater is observed between the oxidized and reduced assignments. In both cases, the oxidized shift is shown within parentheses for comparison. A triple asterisk indicates that a portion of the spin system which is observed in the oxidized form is broadened or otherwise lost in the reduced form. The oxidized assignments are shown in parentheses in this case as well.

manifold are thus paramagnetic, resulting in an increase in the volume surrounding the metal cluster that is affected by line broadening.

The loss of structural data for reduced Pdx caused by the increase in hyperfine broadening is offset to some degree by a gain in information concerning the proximity of certain residues to the metal cluster. The changes in broadening with oxidation state provide information on those residues that are near the edges of the volume affected by the metal cluster. In the oxidized protein, the spin systems of Met 24, Gln 25, Val 36–Val 50, Met 70, Leu 71, Leu 84–Gln 87, and Gln 105 are either partially or completely broadened by proximity to the metal cluster (Ye & Pochapsky, 1992). In the reduced protein, these effects widen to include portions of the spin systems of Ser 22, Leu 23, Ile 35, and interior-facing residues along the α-helix extending from Asn 64 to Cys 73 including Glu 67, Met 70, and Leu 71 and portions of the Val 74, Arg 83, Ile 88, and Val 101 spin systems. On the basis of inspection of the model for the solution structure of oxidized Pdx presented in the accompanying paper, these results represent an increase in teh radius of paramagnetic broadening effects surrounding the metal center by ca. 1 Å.

DQF-COSY connectivity between the Ser 22 $C_\alpha H$ and NH resonances is much weaker in the reduced than in the oxidized protein, and through-bond connectivities from the $C_\alpha H$ to $C_\beta H_2$ protons of Ser 22 are completely lost. A NOE between the $C_\alpha H$ of Ser 22 and the NH of 23 is missing in the reduced form, as are connectivities between the NH, $C_\alpha H$, and $C_\beta H_2$ protons of Leu 23. The Gln 25 $C_\alpha H$ resonance, identified in oxidized Pdx, is missing in the reduced form.

The NH–$C_\alpha H$ COSY connectivity for Ile 35 is absent, although the Ile 35 NH proton is observed, based on sequential NOEs from Asp 34. Connectivity between the $C_\beta H$ and $C_{\gamma 1} H$ resonances of Ile 35 are broadened but still observable in both NOESY and 2QF-COSY spectra.

The spin system of Val 50, which is partially broadened in the oxidized protein, is almost completely missing in the reduced protein; the NH–$C_\alpha H$ COSY connectivity for Val 50 observed in the oxidized protein is gone, and a weak COSY cross peak connects the $C_\beta H$ at 1.79 ppm to one of the $C_\gamma H_3$ methyls at 0.38 ppm.

Residues 65–73 form an α-helix near the metal cluster-binding site. In the oxidized protein, two spin systems in this helix are affected by the paramagnetism of the metal center;

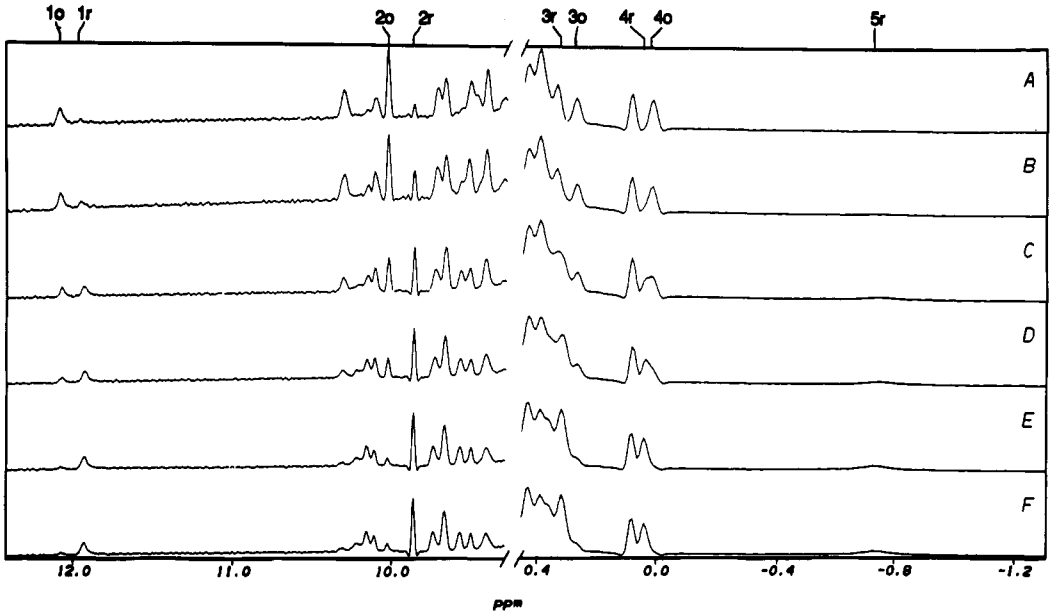

FIGURE 3: Titration of a 0.5-mL sample of a 3 mM sample of oxidized Pdx with 3-μL aliquots of 0.1 M sodium dithionite. Sample is dissolved in 90%/10% H_2O/D_2O, pH 7.4, 290 K. Ratios of oxidized to reduced Pdx (ox%/red%) are approximately as follows: (A) 95/5, (B) 75/25, (C) 50/50, (D) 30/70, (E) 10/90, and (F) 5/95. Assigned resonances are (o = oxidized, r = reduced): 1, His 49 $N_{\delta 1}H$; 2, Trp 106 $N_{\epsilon 1}H$; 3, Ile 32 $C_{\gamma 2}H_3$; and 4, Ile 32 $C_{\delta 1}H_3$. Resonance 5 is unidentified and is observed only in the reduced protein.

only the NH of Met 70 is identified, and the Leu 71 spin system is completely missing. In the reduced protein, the effects of the metal cluster are extended to residue Glu 67 as well. The entire Glu 67 spin system is missing from two-dimensional spectra of reduced Pdx, although a NOE to the NH of Ile 68 is consistent with the assignment of the $C_\alpha H$ of Glu 67 at 4.02 ppm, similar to that for oxidized Pdx. The sequential NOE between the NH of Gly 69 and the NH of Met 70 observed in oxidized Pdx is not visible in spectra of reduced Pdx. One of the $N_\delta H$ amide protons for Asn 64, both of which are observed in the oxidized form, is missing.

The $N_\epsilon H$ resonance of Arg 83 is broader in reduced Pdx relative to the oxidized form, and weaker NOEs are observed to that resonance as well. The NH of Arg 83 is also somewhat broadened, but all side-chain connectivities for Arg 83 are still observed. The entire Gln 87 spin system and portions of Ile 88 are lost in the reduced protein, and some broadening is observed for the side-chain resonance of Val 101. Finally, the $C_\alpha H$ resonance of Gln 105 is broadened in both oxidized and reduced Pdx, although both COSY- and NOESY-type correlations are observed for that resonance in both forms.

NOE and Chemical Shift Changes Unaccompanied by Large Line-Width Changes. Most ^1H chemical shifts for resonances not directly affected by the paramagnetism of the metal center are similar to those observed in oxidized Pdx. Residues forming the major hydrophobic core of the protein show little or no chemical shift or NOE intensity changes as a function of oxidation state of the metal cluster; this is taken as evidence that the structure of this part of the protein does not change significantly in response to redox state. However, as seen from Table 1 and Figures 1 and 2, several regions of the polypeptide show distinct chemical shift differences upon changing oxidation state that are apparently not related to changes in unpaired electron-spin density. These include portions of the α-helix extending from Glu 65 to Cys 73, the loop, Val 74–Leu 78, which connects that helix to the Lys 79–Pro 80–Asn 81–Ser 82 type I turn, and the C-terminal residues, Pro 102–Trp 106. Differences are also observed for the spin systems of His 49 and Tyr 51. Resonances undergoing these shifts are readily identifiable in spectra obtained in the course of a titration of oxidized Pdx with sodium dithionite, shown in Figure 3.

Table 2: NOEs Involving Regions Contiguous with the C-Terminal Peptide (Pro 102–Trp 106) of Reduced Pdx[a]

region	assignment
	Sequential NOEs
Cys 73–Val 74	NH–NH, wm (w); $C_\alpha H$–NH, no (w)
Val 74–Thr 75	NH–NH, no (no); $C_\alpha H$–NH, w (s); $C_\gamma H_3$–NH, w (no)
Thr 75–Ala 76	NH–NH, w (s); $C_\alpha H$–NH, m (wm); $C_\beta H$–NH, vw (w); $C_\gamma H_3$–NH, w (wm)
Ala 76–Glu 77	NH–NH, no (w); $C_\alpha H$–NH, s (s); $C_\beta H_3$–NH, s (s)
Glu 77–Leu 78	NH–NH, m (overlap); $C_\alpha H$–NH, s (s); $C_\beta H_2$–NH, s (s)
Leu 78–Lys 79	NH–NH, w (w); $C_\alpha H$–NH, s (s); $C_\beta H_2$–NH, m (m); $C_\delta H_3$–NH, ms (s)
Pro 102–Asp 103	$C_\delta H_2$–NH, no (m); $C_\alpha H$–NH, ms (s); $C_\beta H_2$–NH, mw (m)
Asp 103–Arg 104	NH–NH, m (ms); $C_\alpha H$–NH, m (s)
Arg 104–Gln 105	NH–NH, no (no); $C_\alpha H$–NH, overlap (s)
Gln 105–Trp 106	NH–NH, s (vs); $C_\alpha H$–NH, ms (s)
	Nonsequential NOEs
His 8 $C_\beta H_2$	Asp 103 $C_\alpha H$, ms (ms); Asp 103 $C_\beta H_2$, mw (ms)
Val 74 $C_\gamma H_3$	Trp 106 $C_\delta H$, ?ms (ms); Trp 106 $N_\epsilon H$, ?ms (m)
Thr 75 $C_\beta H$	Arg 104 $C_\gamma H_2$, w (w); Arg 104 $C_\delta H_2$, w (w); Arg 104 $N_\epsilon H$, no (w)
Thr 75 $C_\gamma H_3$	Arg 104 $C_\delta H_2$, w (w); Arg 104 $N_\epsilon H$, no (w)
Ala 76 $C_\beta H_3$	His 49 $C_{\epsilon 1} H$, ms (ms); His 49 $C_{\delta 2} H$, w (w); His 49 $N_{\delta 1} H$, m (m); Tyr 51 $C_\epsilon H$, m (vw); Pro 102 $C_\beta H_2$, s (ms); Asp 103 NH, w (mw); Arg 104 NH, m (mw)

[a] NOEs are indicated as weak (w), medium (m), strong (s), and not observed (no). Corresponding NOE strengths in the oxidized form are indicated in parentheses. A question mark indicates an assignment which could not be verified by through-bond connectivity.

Inspection of a model for the solution structure of Pdx (see accompanying paper) shows that most of the residues that exhibit chemical shift changes upon reduction are localized in a compact cluster identified by a large number of NOEs between residues His 49, Tyr 51, Val 74, Ala 76, Leu 78, Lys 79, and Ser 82 (Table 2). NOEs observed between residues at the C-terminus of Pdx (Pro 102–Trp 106) and residues Tyr 51, Val 74, Thr 75, and Ala 76 indicate that the C-terminal

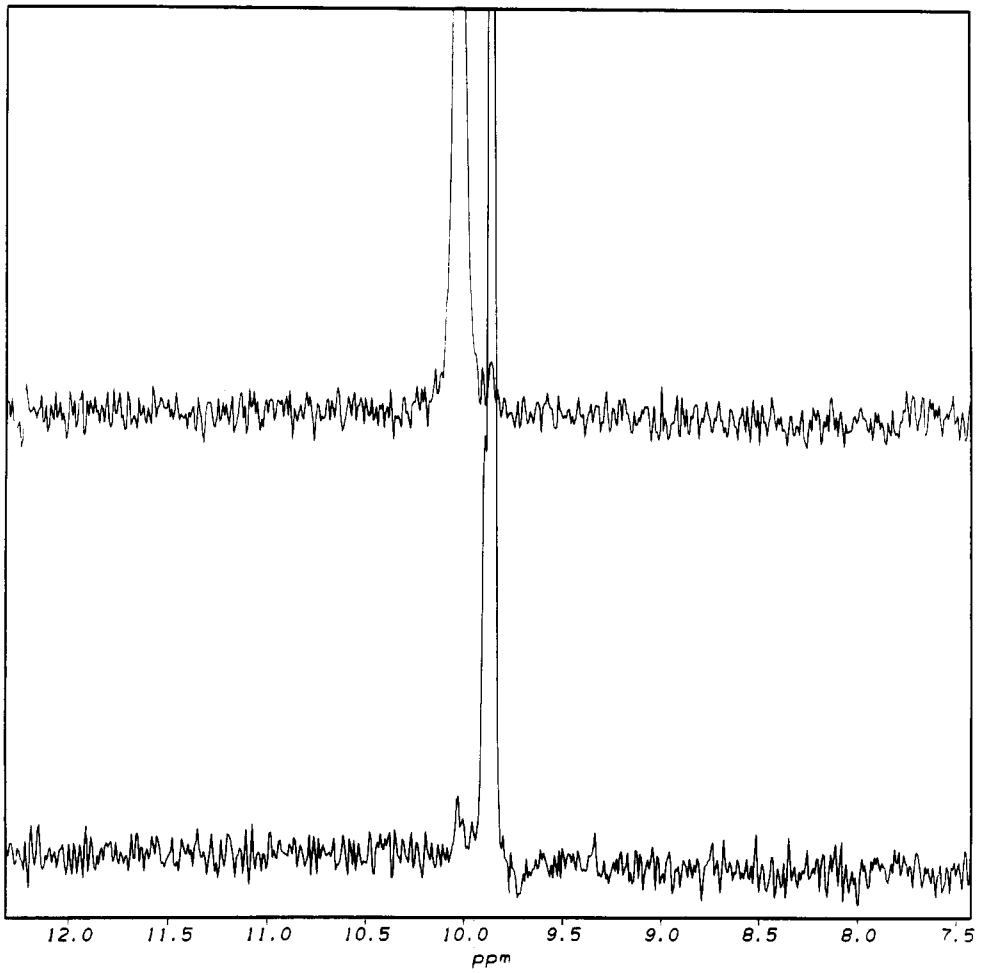

FIGURE 4: Columns extracted from a two-dimensional exchange spectrum of half-reduced Pdx corresponding to the chemical shifts of the $N_{\epsilon 1}H$ proton resonance of Trp 106 in the oxidized (upper) and reduced (lower) forms of Pdx. Mixing time was 100 ms. Symmetric cross peaks due to electron self-exchange can be seen at the chemical shift of the corresponding resonance in both columns. Experiment was obtained with 3 mM total (oxidized plus reduced) protein concentration at 290 K, pH 7.4, in 90%/10% H_2O/D_2O; 400 t_1 values were obtained for the complete experiment with a spectral width of 8064 Hz in both dimensions. Data shown have been zero-filled to 2048 points, with a 90° phase-shifted sine bell applied over all data before zero-filling.

residues also take part in the formation of this compact region. We note that relatively large chemical shift changes are observed at the C-terminal residue itself, Trp 106, upon reduction. The residues in this region of the protein are far enough from the metal center (>10 Å) to discount significant pseudocontact contributions to their shifts, particularly considering the fact that the **g**-tensor of reduced Pdx is nearly isotropic ($\mathbf{g}_\perp$ = 1.94, $\mathbf{g}_\parallel$ = 2.01) (Tsibris et al., 1968). The pseudocontact shift exhibits an r^{-3} dependence on the distance between the paramagnetic center and the observed spin and linear dependence on the difference between $\mathbf{g}_\perp$ and $\mathbf{g}_\parallel$ (McConnell & Robertson, 1958). The high symmetry of the **g**-tensor makes significant pseudocontact shifts in the reduced protein unlikely except for residues quite close to the metal center (Phillips & Poe, 1973).

This region of the protein also exhibits changes in NOE intensities upon reduction of the metal center. These intensity differences are particularly noticeable for the resonances of Thr 75 and Ala 76, which also show significant chemical shift variances between the two forms (see Tables 1 and 2).

Electron Exchange in Half-Reduced Samples of Pdx. Spectra of half-reduced samples of Pdx (Figure 3) demonstrate that electron self-exchange in partially reduced samples of Pdx is slow on the ^1H chemical shift time scale. NOESY spectra obtained as a function of mixing time on half-reduced samples of Pdx do not show exchange cross peaks at mixing times less than 100 ms. Using a 100-ms NOESY mixing time with a 3 mM total (oxidized plus reduced) protein concentration, exchange cross peaks are observed in the NOESY between resonances of oxidized and reduced Pdx that are ~1% of the intensity of the corresponding diagonal peaks (Figure 4). Using this value to estimate an exchange rate (i.e., one out of every 100 molecules of reduced Pdx will reoxidize in 0.1 s) yields a *maximum* value for the second-order rate constant for electron self-exchange in Pdx of 66 M^{-1} s^{-1}.

DISCUSSION

Placement of the Metal Cluster in Pdx. Paramagnetic broadening in oxidized Pdx makes the sequential assignment of resonances corresponding to nuclei nearer than ca. 8 Å to the metal cluster impossible using standard methods. In order to integrate NOE and dihedral angle constraints for the diamagnetic regions of the protein into a reasonable solution structure for Pdx, it is, at present, necessary to model the metal cluster-binding site upon known metal cluster structures in other ferredoxins and model compounds. However, differences in hyperfine interactions between oxidized and reduced Pdx do provide some information concerning the position of the metal cluster in the protein structure with respect to structural features that can be identified. The spatial distribution of these effects is shown in Figure 5. Observations of differential broadening between the oxidized and reduced

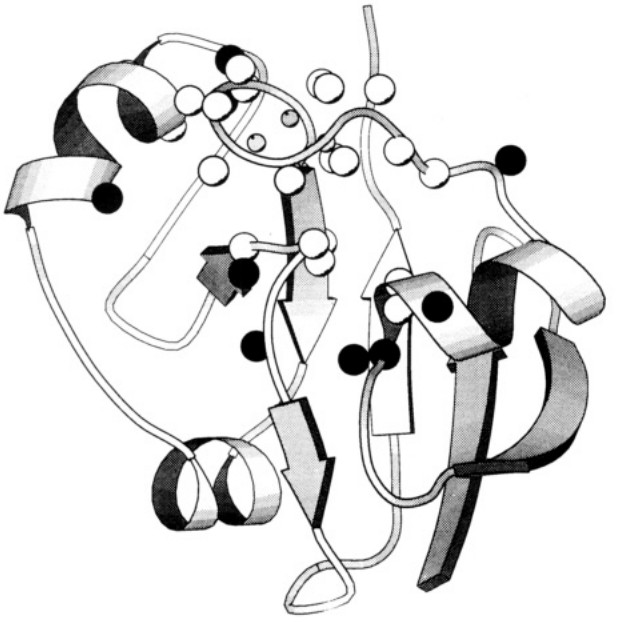

FIGURE 5: Spatial distribution of paramagnetic broadening in the oxidized and reduced forms of Pdx. White spheres represent amino acid residues containing resonances which cannot be identified in either the oxidized or reduced protein, while dark spheres represent residues containing resonances which are observed in the oxidized but not reduced form. The iron–sulfur cluster atoms are shown as smaller shaded spheres. Perspective is the same as in Figure 4 of the accompanying paper.

forms of Pdx have been used to loosely constrain the position of the metal cluster within the protein in structural calculations, as discussed in detail in the accompanying paper.

Structural Constraints on the C-Terminal Region of Pdx and Modeling of the Structure of Reduced Pdx. The critical role of the C-terminal residue of Pdx, Trp 106, in the interaction between Pdx and cytochrome P-450$_{cam}$ has been the subject of much discussion and experimentation. It was observed that Pdx from which Trp 106 has been removed either by mutagenesis or by carboxypeptidase treatment exhibits greatly decreased activity, although the metal cluster (and by inference, the tertiary structure of the protein) remains intact and reduction potentials are unchanged (Sligar et al., 1974; Davies et al., 1990; Davies & Sligar, 1992). There has been speculation that the π-electrons of aromatic functionality may provide a low-resistance pathway for electron transfer in proteins, although little evidence is available to support this proposal (Everest et al., 1991). Recently, Baldwin considered electron transfer between Pdx and P-450$_{cam}$ in terms of a covalent bond switching involving the Trp 106 indole and one of the cysteinyl sulfurs which ligates the Fe–S cluster (Baldwin et al., 1991). However, this mechanism is not consistent with published data on kinetic and thermodynamic parameters for several C-terminal mutants of Pdx, which show that the primary role of the C-terminal residue is to mediate binding with P-450$_{cam}$ (Davies & Sligar, 1992). In a detailed thermodynamic and kinetic analysis of a series of C-terminal mutants of Pdx, these workers demonstrated that the presence of tryptophan at this position significantly stabilizes the one-electron-reduced complex between Pdx and P-450$_{cam}$ and that other aromatic residues may substitute to some extent in this role. We note in passing that the stabilization of protein–protein and protein–substrate complexes is a role assumed by aromatic residues in many cases (Pochapsky & Gopen, 1992).

A significant number of NOE constraints on the C-terminal residues of Pdx have now been identified (Table 2). NOEs between the $C_\beta H_3$ protons of Ala 76 and the NH protons of

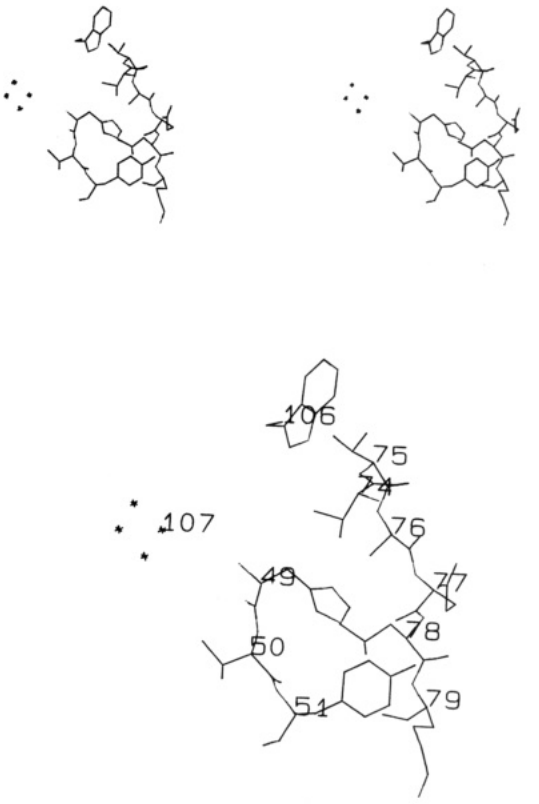

FIGURE 6: C-terminal region of Pdx, including residues His 49, Val 50, Tyr 51, Val 74, Thr 75, Ala 76, Glu 77, Leu 78, Lys 79, Pro 102, Asp 103, Arg 104, Gln 105, and Trp 106. The position of the metal cluster is also indicated (residue 107). Residues in this region show the largest chemical shift and NOE changes upon reduction. The top portion of the figure is a stereoview of the lower, numbered figure.

Asp 103 and Arg 104, NOEs between the ring protons of Tyr 51 and Ala 76 and the spin system of Pro 102, and those between the side chain of Arg 104 and Thr 75 constrain this portion of the polypeptide. Using these constraints, the structure of the C-terminal region of Pdx has been characterized as shown in Figure 6.

Only two interresidue NOEs are observed for the indole ring of Trp 106 in oxidized Pdx, and these are observed only at the $C_{\delta 1}H$ and $N_{\epsilon 1}H$ protons (on the five-membered ring of the indole). The $C_\gamma H_3$ of Val 74 gives rise to a NOE at both the $C_{\delta 1}H$ and $N_{\epsilon 1}H$ protons of Trp 106. The other NOE, observed for the $N_{\epsilon 1}H$ proton, was previously assigned to a methyl group of Val 98 (Ye et al., 1992). However, this NOE has since been shown to be due to a resonance that overlaps the Val 98 methyl resonance and remains unidentified because of a lack of observable through-bond connectivity. The line width of this resonance is suggestive of a methyl group, and the structural model indicates that it could be the $C_\beta H_3$ of Ala 46 (which has not been assigned sequentially due to the broadening of nearby residues by hyperfine interactions but which the present structural models suggest is further than 8 Å from the nearest iron atom). The lack of NOEs for the remainder of the indole ring protons indicates that the six-membered benzyl ring of the indole moiety is surface exposed and only the five-membered pyrrole structure interacts with other residues, perhaps due to the presence of a "cleft" on the surface of the protein into which the five-membered ring inserts but from which the six-membered ring extends. Nonselective ^1H T_1 measurements for the Trp 106 $C_{\delta 1}H$ resonance (180 +/−10 ms for reduced Pdx, 308 +/−10 ms for the oxidized form) are consistent with the Trp 106 indole being marginally affected by paramagnetic relaxation. The position of the indole

ring in Figure 6 places the $C_{\delta 1}H$ proton about 10 Å from the nearest iron atom of the metal cluster. However, the structure presented is likely to be biased toward conformations of the C-terminal Trp that give rise to interresidue NOEs (see accompanying paper). Evidence obtained by other workers for conformational heterogeneity of the Trp 106 indole suggests that the structure shown presents only one of several conformers occupied by this residue (Stayton & Sligar, 1991). Some of these conformers may place the indole ring further than 10 Å from the metal center.

As noted above, the indole protons of Trp 106 display large differences in chemical shift between the two redox states. The patterns of NOEs for the Trp 106 indole protons in the oxidized protein are maintained in reduced Pdx, but the chemical shifts of the resonances with which these NOEs occur are shifted dramatically (by –0.30 ppm for the Val 74 methyl and –0.39 ppm for the unidentified methyl group). Lacking complete assignments for Val 74 in reduced Pdx, it cannot be concluded with certainty that the NOEs observed for the indole ring protons in the reduced form are due to the same resonances as in the oxidized protein, although this seems likely, as the assignments of NOEs for other resonances near the C-terminus are the same in both forms.

If Trp 106 marks the region of the Pdx surface to which $P\text{-}450_{cam}$ binds, it is of interest to note those residues that are nearby on the surface of the protein and likely to be involved in the interactions with $P\text{-}450_{cam}$. A number of charged groups are located in the vicinity of Trp 106 on the surface of the protein, including His 8, Asp 9, Asp 38, Glu 77, Lys 79, Asp 100, Asp 103, and Arg 104. NOEs between the side chains of His 8 and Asp 103 (Table 2) are suggestive of an ionic interaction between these two residues. With the exception of Glu 77, all of these residues are among those showing chemical shift differences between the oxidized and reduced forms. As previously described, a hydrophobic "patch" consisting of the side chains of Val 4, Val 6, and Val 98 may also provide part of the binding surface (see accompanying paper).

Incorporation of observed changes in NOE intensities into simulated annealing protocols of the type described in detail in the accompanying paper generated structures for the reduced protein in which the mean structures differ slightly in their backbone atom positions from the structure of oxidized Pdx, particularly between Ala 62–Lys 79 and Pro 102–Trp 106. However, the largest differences between calculated structures of oxidized and reduced Pdx occur in regions where there are relatively few interdomain NOE constraints (Ala 62–Val 74), so it is not clear that these differences can be interpreted meaningfully at present. A much larger number of structures must be generated using more constraints in order to structurally characterize in detail the conformational differences between the two oxidation states of Pdx. Such calculations must, in turn, await the availability of heteronuclear-edited multidimensional NOESY data on both forms.

CONCLUSIONS

Chemical shift changes observed upon changing redox state in Pdx that are not caused by hyperfine interactions are for the most part localized to those residues spatially close to the C-terminus. Changes in NOE patterns are observed primarily for the C-terminal Trp 106, the indole protons of which experience the largest confirmed chemical shift change upon reduction of Pdx, and for the Val 74–Ala 76 loop. The upfield shifts of the resonances that give rise to the NOEs observed for the Trp 106 $N_{\epsilon 1}H$ and $C_{\delta 1}H$ protons (one of which is probably the $C_\gamma H_3$ methyl of Val 74) in the reduced protein are consistent with the increased burial of a portion of the indole ring or the indole moiety spending a larger fraction of total time in a conformation that gives rise to the observed shielding effects. The upfield shifts of the indole proton resonances in the reduced protein are also consistent with decreased solvation in the reduced form (Lambert et al., 1976).

How Are Oxidation State, Midpoint Potential, and P-450 Binding Coupled in Pdx? Resonance Raman studies of a variety of reduced Fe_2S_2 ferredoxins confirm that there is a high degree of structural similarity between the metal clusters of these proteins (Han et al., 1989; Fu et al., 1992). Despite these similarities, the redox potentials of two-iron ferredoxins cover a significant range. The plant-type ferredoxins have midpoint potentials ranging from –310 to –455 mV (Knaff & Hirasawa, 1991). Mammalian adrenodoxin, which transfers electrons to $P\text{-}450_{scc}$ in a fashion analogous to that of the $Pdx/P\text{-}450_{cam}$ couple, has a midpoint potential of –250 mV (Jefcoate, 1986). Free Pdx, as noted above, has a midpoint potential of –230 mV and, upon binding to $P\text{-}450_{cam}$, changes potential to –196 mV. Clearly, environmental effects are critical in determining the redox behavior of the metal cluster.

The observed structure of a protein is thought to represent a weighted average of populated conformational substates (CS) which are separated by low energetic barriers (Austin et al., 1975; Frauenfelder et al., 1979). The observed midpoint potential of a redox protein should therefore be a weighted average of the midpoint potentials of each occupied CS in the vicinity of the redox center, and a change in the relative populations of CS should result in a change in the observed midpoint potential. Conversely, a change in oxidation state would preferentially populate those CS that favor the product state. The effect of such population shifts would be observed in NMR spectra as changes of chemical shifts and NOE intensities (assuming that equilibration is fast on the NMR time scale). Interestingly, EPR line-width dependence on field strength for reduced spinach ferredoxin has been tentatively attributed to "*g* strain," that is, the existence of a distribution of *g* values indicating a distribution of conformers (Orme-Johnson & Sands, 1973).

Differences between the CS occupied preferentially by one or the other oxidation state may have long-range effects. Cytochrome b_5 shows a greatly reduced rate of interconversion between heme orientational isomers in the reduced form relative to the oxidized form (Pochapsky et al., 1990). Cytochrome *c* also shows marked changes in physical properties as a function of oxidation state (Feng et al., 1990; Liu et al., 1989). The oxidation state of the metal cluster in Pdx is clearly affecting conformation in regions well removed from it (in the model shown in Figure 6, the $C_\gamma H_3$ of Thr 75 is 14.5 Å from the nearest iron atom). It is interesting to speculate that reduced Pdx might populate a subset of the CS populated by oxidized Pdx. If the same subset of CS populated in the reduced protein is also that which binds most efficiently to $P\text{-}450_{cam}$, a mechanism for coupling oxidation state and binding affinity is available. Conversely, complexation of oxidized Pdx by $P\text{-}450_{cam}$ will decrease the degrees of conformational freedom available, reducing the number of occupied CS to that which favors the bound form. If this is the same subset of CS that is populated by reduced Pdx, the midpoint potential of $P\text{-}450_{cam}$-bound Pdx relative to free Pdx should be affected, as is in fact observed, by becoming more positive.

Experimental tests of this hypothesis are possible. Amide-proton-exchange rates will provide information regarding dynamic differences between the oxidized and reduced Pdx;

these experiments are in progress. Finally, if reduced Pdx is less mobile (occupies fewer CS) than the oxidized form, this should be reflected in the temperature dependence of the relative binding affinities of oxidized and reduced Pdx for cytochrome P-450$_{cam}$, as well as in the temperature dependence of the midpoint potential of Pdx.

ACKNOWLEDGMENT

The authors thank Xiao Mei Ye for access to the oxidized Pdx assignments and Susan Sondej Pochapsky (Bruker Instruments) for providing the 600-MHz data shown here. We also thank S. G. Sligar for helpful discussion.

SUPPLEMENTARY MATERIAL AVAILABLE

^{1}H assignments for reduced putidaredoxin, pH 7.4, 10 mM Tris, 290 K (4 pages). Ordering information can be obtained from any current masthead page.

REFERENCES

Austin, R. H., Beeson, K. W., Eisenstein, L., Frauenfelder, H., & Gunsalus, I. C. (1975) *Biochemistry 14*, 5355.

Baldwin, J. E., Morris, G. M., & Richards, W. G. (1991) *Proc. R. Soc. London, B 245*, 43–51.

Banci, L., Bertini, I., & Luchinat, C. (1990) *Structure and Bonding 72*, Springer-Verlag, Berlin, Heidelberg.

Billeter, M., Braun, W., & Wurthrich, K. (1982) *J. Mol. Biol. 155*, 321–346.

Cushman, D. W., Tsai, R. L., & Gunsalus, I. C. (1967) *Biochem. Biophys. Res. Commun. 26*, 577.

Davies, M. D., & Sligar, S. G. (1992) *Biochemistry 31*, 11838–11389.

Davies, M. D., Qin, L., Beck, J. L., Suslick, K. S., Koga, H., Horiuchi, T., & Sligar, S. G. (1990) *J. Am. Chem. Soc. 112*, 7396–7398.

Feng, Y., Roder, H., & Englander, S. W. (1990) *Biochemistry 29*, 3494–3504.

Frauenfelder, H., Petsko, G. A., & Tsernoglou, D. (1979) *Nature 280*, 558.

Fu, W., Drozdzewski, P. M., Davies, M. D., Sligar, S. G., & Johnson, M. K. (1992) *J. Biol. Chem. 267*, 15502–15510.

Gerber, N. C., Horiuchi, T., Koga, H., & Sligar, S. G. (1990) *Biochem. Biophys. Res. Commun. 169*, 1016–1020.

Han, S., Czernuszewicz, R. S., Kimura, T., Adams, M. W. W., & Spiro, T. G. (1989) *J. Am. Chem. Soc. 111*, 3505–3511.

Hintz, M. J., Mock, D. M., Peterson, L. L., Tuttle, K., & Peterson, J. A. (1982) *J. Biol. Chem. 257*, 14324–14332.

Hughes, M. N. (1972) *The Inorganic Chemistry of Biological Processes*, Chapter 3, pp 152–154, John Wiley and Sons, London.

Jefcoate, C. R. (1986) in *Cytochrome P-450, Structure, Mechanism and Biochemistry* (Ortiz de Montellano, P. R., Ed.) Plenum Press, New York.

Knaff, D. B., & Hirasawa, M. (1991) *Biochim. Biophys. Acta 1056*, 93–125.

Koga, H., Yamaguchi, E., Matsunaga, K., Aramaki, H., & Horiuchi, T. (1989) *J. Biochem. (Tokyo) 106*, 831–836.

Kraulis, P. J. (1991) *J. Appl. Crystallogr. 24*, 946–950.

Kumar, A., Ernst, R. R., & Wuthrich, K. (1980) *Biochem. Biophys. Res. Commun. 95*, 1–6.

Lambert, J. B., Shurvell, H. F., Verbit, L., Cooks, R. G., & Stout, G. H. (1976) *Organic Structural Analysis*, pp 44–45, Macmillan Publishing Co., New York.

Liu, G., Grygon, A., & Spiro, T. G. (1989) *Biochemistry 28*, 5046.

Mayerle, J. J., Denmark, S. E., DePamphilis, B. V., Ibers, J. A., & Holm, R. H. (1975) *J. Am. Chem. Soc. 97*, 1032–1045.

McConnell, H. M., & Robertson, R. (1958) *J. Chem. Phys. 29*, 136.

McLendon, G. (1988) *Acc. Chem. Res. 21*, 160–167.

Miura, S., & Ichikawa, Y. (1991) *J. Biol. Chem. 266*, 6252–6258.

Nilges, M., Gronenborn, A. M., & Clore, G. M. *FEBS Lett. 229*, 317–324.

Oh, B.-H., & Markley, J. L. (1990) *Biochemistry 29*, 3993–4004.

Phillips, W. D., & Poe, M. (1973) in *Iron Sulfur Proteins* (Lovenberg, W., Ed.) Vol. II, pp 255–284, Academic Press, New York.

Pochapsky, T. C., & Ye, X. M. (1991) *Biochemistry 30*, 3850–3856.

Pochapsky, T. C., & Gopen, Q. (1992) *Protein Sci. 1*, 786–795.

Pochapsky, T. C., Sligar, S. G., McLachlan, S. J., & La Mar, G. N. (1990) *J. Am. Chem. Soc. 112*, 5258–5263.

Pochapsky, T. C., Ye, X. M., Ratnaswamy, G., & Lyons, T. A. (1994) *Biochemistry* (preceding paper in this issue).

Poulos, T. L., Finzel, B. C., & Howard, A. J. (1987) *J. Mol. Biol. 195*, 687–700.

Rance, M., Sorensen, O. W., Bodenhausen, G., Wagner, G., Ernst, R. R., & Wuthrich, K. (1983) *Biochem. Biophys. Res. Commun. 117*, 458–479.

Rance, M., Chazin, W., Dalvit, C., & Wright, P. E. (1989) *Methods Enzymol. 176*, 114–134.

Ratnaswamy, G., & Pochapsky, T. C. (1993) *Magn. Reson. Chem. 31* (in press).

Rypniewski, W. R., Breiter, D. R., Benning, M. W., Wesenberg, G., Oh, B.-H., Markley, J. L., Rayment, I., & Holden, H. M. (1991) *Biochemistry 30*, 4126–4131.

Sligar, S. G., & Gunsalus, I. C. (1976) *Proc. Natl. Acad. Sci. U.S.A. 73*, 1078–1082.

Sligar, S. G., & Murray, R. I. (1986) in *Cytochrome P-450, Structure, Mechanism and Biochemistry* (Ortiz de Montellano, P. R., Ed.) Chapter 12, Plenum Press, London.

Sligar, S. G., DeBrunner, P. G., Lipscomb, J. D., & Gunsalus, I. C. (1974a) *Int. Conf. Biochem. 9th*, Abstr. 7c12, p 339.

Sligar, S. G., DeBrunner, P. G., Lipscomb, J. D., Namtvedt, M. J., & Gunsalus, I. C. (1974b) *Proc. Natl. Acad. Sci. U.S.A. 71*, 3906–3910.

Stayton, P. S., & Sligar, S. G. (1991) *Biochemistry 30*, 1845–1851.

Tsibris, J. C. M., Tsai, R. L., Gunsalus, I. C., Orme-Johnson, W. H., Hansen, R. E., & Beinert, H. (1968) *Proc. Natl. Acad. Sci. U.S.A. 59*, 959–965.

Tsukihara, T., Fukuyama, K., Nakamura, M., Katsube, Y., Tanaka, N., Kakudo, M., Wada, K., Hase, T., & Matsubara, H. (1983) *J. Biochem. 90*, 1763–1773.

Tsukihara, T., Fukuyama, K., Mizushima, M., Harioka, T., Kusunoki, M., Katsube, Y., Hase, T., & Matsubara, H. (1990) *J. Mol. Biol. 216*, 399–410.

Wuthrich, K. (1986) *NMR of Proteins and Nucleic Acids*, John Wiley and Sons, New York.

Wuthrich, K., Billeter, M., & Braun, W. (1983) *J. Mol. Biol. 169*, 949–961.

Ye, X. M., Pochapsky, T. C., & Pochapsky, S. S. (1992) *Biochemistry 31*, 1961–1968.